Fast-ion redistribution and loss due to edge perturbations in the ASDEX Upgrade, DIII-D and KSTAR tokamaks

M. García-Muñoz[1], S. Akaslampolo[2], O. Asunta[2], J. Boom[3], X. Chen[4], I. G. J. Classen[3], R. Dux[1], T. E. Evans[5], S. Fietz[1], R. K. Fisher[5], C. Fuchs[1], B. Geiger[1], W. W. Heidbrink[4], M. Hoelzl[1], V. Igochine[1], J. Kim[6], J. Y. Kim[6,7], T. Kurki-Suonio[2], B. Kurzan[1], N. Lazányi[8], N. Luhmann[9], T. Lunt[1], R. M. McDermott[1], M. Maraschek[1], M. Nocente[10,11], H. Park[12], G. I. Pokol[8], D. C. Pace[5], T. L. Rhodes[13], K. Shinohara[14], W. Suttrop[1], M. A. Van Zeeland[5], E. Viezzer[1], M. Willensdorfer[15], E. Wolfrum[1]
and the ASDEX Upgrade, DIII-D and KSTAR Teams

[1] Max-Planck-Institut für Plasmaphysik, EURATOM Association, D-85748, Germany
[2] Aalto University, FI-00076 AALTO, FINLAND
[3] FOM Institute DIFFER* - Association EURATOM-FOM, 3430 BE, The Netherlands
[4] University of California-Irvine, Irvine, California 92697, USA
[5] General Atomics, San Diego, California, 92186-5608, USA
[6] National Fusion Research Institute, Daejeon 169-148, Korea
[7] University of Science and Technology, Daejeon 305-350, Korea
[8] BME NTI, Association EURATOM, Pf 91, H-1521 Budapest, Hungary
[9] University of California-Davis, Davis, California 95616,USA
[10]Università degli Studi di Milano-Bicocca, 20126, Milano, Italy
[11] Istituto di Fisica del Plasma "Piero Caldirola" EURATOM- ENEA-CNR, 20125, Milan, Italy
[12] POSTECH, Pohang, Gỳeongbuk, 790-784, Korea
[13] University of California-Los Angeles, Los Angeles, California 90098, USA
[14] JAEA, 801-1, Mukouyáma, Naka City, Ibaraki, 311-0193, Japan
[15] Technische Universität Wien, Association EURATOM-ÖAW, Vienna, Austria

e-mail: Manuel.Garcia-Munoz@ipp.mpg.de

Abstract. The impact of Edge Localized Modes (ELMs) and externally applied Resonant and Non-Resonant Magnetic Perturbations (MPs) on fast-ion confinement / transport have been investigated in the ASDEX Upgrade, DIII-D and KSTAR tokamaks. These studies were enabled by coordinated multi-machine experiments and new diagnostic capabilities that provide detailed information on the interaction between energetic particles and instabilities in particle phase-space. Filament-like bursts of fast-ion losses induced by ELMs dominate the losses in H-mode plasmas as measured by fast-ion loss detectors (FILDs) at different toroidal and poloidal positions. In low-collisionality H-modes, ELM and inter-ELM fluctuations in fast-ion losses are often strongly connected with main ELM properties and edge flows. Filamentary fast-ion losses are observed during ELMs, suggesting a strong interaction between fast-ions and the instabilities concomitant to the ELM cycle, blobs and filaments. Large changes in escaping-ion phase-space are observed within a single ELM. Externally applied MPs have little effect on kinetic profiles, including fast-ions, in high collisionality plasmas with mitigated ELMs while a strong impact on kinetic profiles is observed in low-collisionality, low q_{95} plasmas with resonant and non-resonant MPs. During the mitigation / suppression of type-I ELMs by externally applied MPs, the large fast-ion blobs / filaments observed during ELMs are replaced by a loss of fast-ions with a broad-band frequency and an amplitude of up to an order of magnitude higher than the NBI prompt loss signal without MPs; a clear synergy in the overall fast-ion transport is observed between MPs and Neoclassical Tearing Modes (NTMs). Measured fast-ion losses show a broad energy and pitch-angle range and are typically on banana orbits that explore the entire pedestal / Scrape-Off-Layer (SOL). The fast-ion response to externally applied MPs presented here may be of general interest for the community to better understand the MP field penetration and overall plasma response. Full orbit simulations indicate that MPs push the loss boundary radially inwards opening and populating the loss cone with particles that would be otherwise well confined.

1. Introduction

High confinement regimes in tokamak plasmas [1] are characterized by Edge Transport Barriers (ETBs) [2] that develop rather steep edge pressure gradients ∇p, which destabilize large-scale Edge Localized Modes (ELMs) [3] causing intermittent relaxation of edge kinetic profiles. ELM induced heat loads on plasma facing components will likely be intolerable in ITER [4,5]. This could actually be the case for inter-ELM cross-field transport too [6]. The successful realization of fusion relies, therefore, in a thorough understanding of edge stability and ELM control. In theory, ELMs can be avoided if the averaged ∇p, is reduced by widening the steep gradient region [7]. In present fusion devices, this is obtained through externally applied resonant and non-resonant magnetic perturbations (MPs) [8-11]. MPs have demonstrated their potential to mitigate/suppress ELMs as well as to control Resistive Wall Modes (RWM) [12], Neoclassical Tearing Modes (NTMs) [13] and plasma rotation [14]. However, results obtained in different machines are not always clearly aligned, e.g. rotation in high-density plasmas in AUG and DIII-D, which emphasizes the importance of taking into account the plasma response when interpreting the effects of 3D externally applied MPs. Indeed, the plasma response is a key ingredient in determining the stability evolution as the plasma can amplify, suppress or modify a perturbation. Extensive theoretical, modeling and computational efforts have led to an enormous progress. However, neither standard fluid simulations based on the baseline plasma transport theory in stochastic magnetic fields [15] nor the most advanced two-fluids, kinetic nor hybrid simulations have successfully explained the full ELM cycle nor the plasma response to externally applied MPs, especially when anomalous transport needs to be considered self-consistently [16,17]. Kinetic effects become of special importance to assess plasma stability in low collisionality burning plasmas with a significant suprathermal (fast) ion content. Fast-ions are indeed an essential source of momentum and energy that under certain conditions may drive directly, or contribute to the development of some, MHD fluctuations that may, in turn, have deleterious effects on global plasma confinement parameters. While kinetic effects of thermal plasma (ions) have been recognized as an important ingredient in the ELM cycle and its mitigation through MPs, little effort have been invested so far in including a kinetic treatment of fast-ions in modeling and computational tools. This is, in part, certainly due to the lack of accurate fast-ion measurements in the area of interest ($\rho_{pol} > 0.6$) as well as associated losses with ELMs and MPs.

In this paper we will present the latest experimental results obtained in AUG, DIII-D and KSTAR on ELM and MP induced fast-ion dynamics. The intermittent transport of thermal plasma across the SOL differs significantly from the results presented here, as expected due to their very different orbital time and length scales, and is presented elsewhere [18]. As a result of a collaborative work on energetic particles, the AUG, DIII-D and KSTAR tokamaks are now equipped with a set of state-of-the-art fluctuations and fast-ion diagnostics such as scintillator based Fast-Ion Loss Detectors (FILDs) [19-21] and Fast-Ion D-Alpha (FIDA) spectroscopy systems [22,23]. Large bandwidth FILD units have shown the strong impact that ELMs and MPs may have on fast-ion losses in escaping ion velocity-space revealing, at the same time, important details on inter- and intra-ELM fluctuations. Active FIDA measurements have been used to monitor the temporal evolution of confined fast-ions during ELMs and MP mitigated ELMy phases. Passive FIDA and Neutral Particle Analyzer (NPAs) are typically used to complement FILD signals with independent measurements of fast-ion losses. Internal fluctuation

measurements are provided by Electron Cyclotron Emssion- (ECE), Imaging (ECE-I), Soft X-Ray (SXR) and reflectometry diagnostics.

2. ELM induced fast-ion losses

ELM-induced fast-ion losses have been studied in the AUG, DIII-D and KSTAR tokamaks at different positions with a set of FILD systems in plasmas with different collisionalities, β_N, and q_{95}. Two phases can be clearly distinguished in ELM induced fast-ion losses with respect to the ELM cycle (inter- and intra-ELM losses). Both phases have been highlighted in grey and black in Fig.1-(b) and are described in the next two paragraphs.

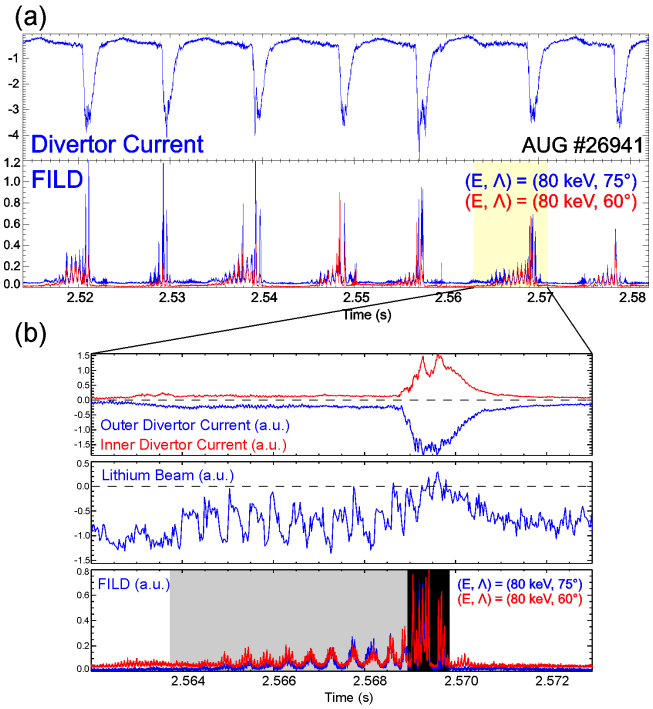

Fig.1. AUG discharge #26941. Fast-ion losses during ELM cycle and correlation with edge density fluctuations. (a) Time traces of fast-ion losses and measured divertor currents at outer divertor plate. (b) Divertor currents at inner (red) and outer (blue) targets, density fluctuations at separatrix (Li-beam) and FILD signals.

Inter-ELM losses. In AUG and DIII-D low-density H-modes, a coherent modulation of the edge density, observed often just before the ELM crash, is correlated with a fast-ion loss (the amplitude of which increases towards the ELM crash). The pre-ELM density fluctuation is measured in AUG with high spatio-temporal resolution by means of the Lithium beam diagnostic. Fig.1 gives an overview of such a phase with the measured divertor current as ELM monitor, the edge density fluctuation measured by Lithium beam and the fast-ion losses with energies E ~ 80 keV and two different pitch angles 60° and 70°. Fig.1-(a) shows a time window with several ELMs where the increasing losses towards the ELM crashes are clearly visible. A zoom of an ELM cycle, Fig.1-(b), shows a clear phase-correlation between the measured fluctuations in Li-Beam and the pre-ELM fast-ion losses. It is worth to note that the amplitude of the measured fast-ion losses grows towards the ELM crash while the amplitude of the density fluctuation remains at a rather constant value. In DIII-D, Doppler backscattering reflectometry shows a similar correlation between the oscillations in the fast-ion losses and those in the pedestal flows, indicating a possible effect of a

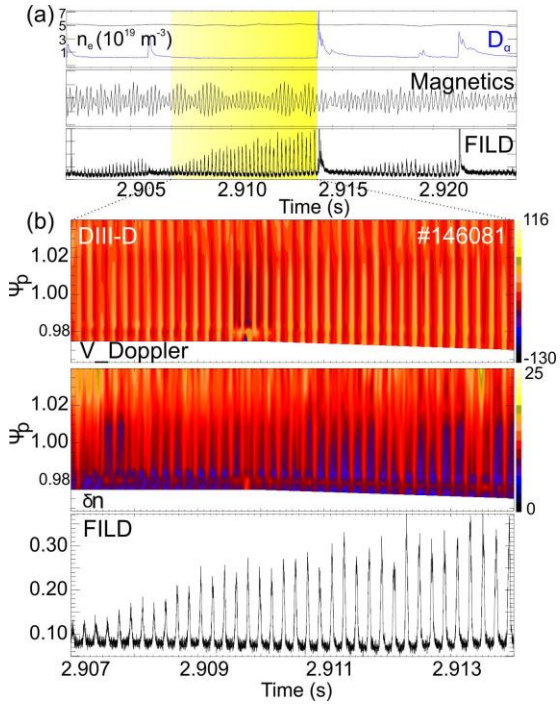

Fig.2. DIII-D discharge #146081. Fast-ion losses during ELM cycle and correlation with edge flow. (a) Time traces of density, D_α, magnetics and FILD. (b) Backscattering doppler reflectometry velocity, density fluctuations and fast-ion losses.

non-ambipolar particle flux on the radial electric field (E_r), see Fig.2. The velocity-space of the escaping ions measured with the DIII-D midplane FILD (FILD2) is shown in Fig.3-(a). In general, pre-ELM losses appear typically in a region that corresponds to deuterium ions with energies between 45 keV in DIII-D (with maximal injection energy E_{NBI} = 80 keV) and 80 keV for AUG (with E_{NBI} = 93 keV) and pitch-angles between 60° and 85°. Fig.3-(b) and -(c) show a typical measured fast-ion trajectory traced backwards in time from FILD2 to the plasma in a DIII-D EFIT equilibrium. No overlapping between the ion trajectory and the NBI footprint is observed indicating that the observed losses are not NBI prompt losses due to a change in the density of the pedestal / SOL during the ELM cycle.

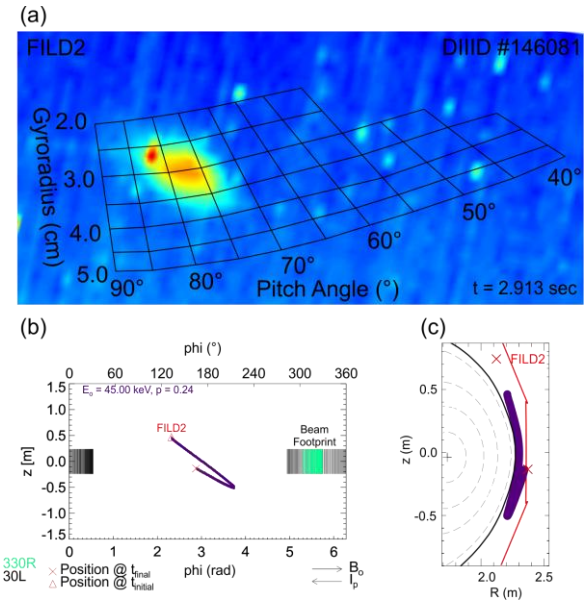

Fig.3. DIII-D discharge #146081. Orbit topology of escaping ions during ELMs measured with FILD2 at DIIID.

Intra-ELM losses. The fast-ion losses associated to the highly non-linear phase of an ELM cycle (crash and post-crash) are studied in 3D with an array of FILD systems located at different toroidal and poloidal positions in AUG and DIII-D. ELM induced fast-ion losses are also measured with passive FIDA as well as Neutral Particle Analyzers (NPA). Overall, FILD measures bursting ELM-induced fast-ion losses that are an order of magnitude higher than any other MHD induced fast-ion loss. Surprisingly, in low collisionality H-modes, inter-ELM fluctuations in fast-ion losses appear connected with basic ELM properties (amplitude and frequency), i.e. high frequency small ELMs are often accompanied by large fluctuating fast-ion losses. Well-defined bursts of fast-ion losses are observed with type-I ELMs, suggesting a strong interaction between fast-ions and the fluctuations concomitant to the ELM crash and subsequent blobs / filaments. In AUG, with 2 FILD units located ~ 30 cm above the midplane and 113° apart toroidally, most of the bursts are measured simultaneously by both detectors, indicating the toroidal and poloidal extention of the loss mechanism and particle source. In this regard, as introduced in the previous section, no correlation is found with the density flush in the pedestal / SOL following the ELM crash. 1D and 2D fast ECE diagnostics provide the best correlation with the fast-ion losses giving important information on the internal fluctuations that may have originated the fast-ion losses. Most important losses are observed in low collisionality type-I ELMs. This is, in fact, expected from the peeling-ballooning theory where the ELM radial extension depends, among other parameters, on pedestal density / collisionality [7]. Up to 5-6 fast-ion bursts are observed at each type-I ELM with each burst lasting for ~ 0.2 ms at FWHM and with ~ 0.2 ms between fast-ion bursts. In escaping-ion velocity-space, bursts within a single ELM often show significant changes in the energy and pitch angle of the lost ions while most of the escaping ions are on trapped orbits with energies E ~ 80 keV.

3. MP induced fast-ion dynamics

The fast-ion dynamics induced by MPs have been studied in the AUG and KSTAR tokamaks in H-mode plasmas with a wide range of collisionalities. In AUG, ELM mitigation by 3D externally applied MPs is achieved above a certain density, ~ 0.6 n_{GW} and a rather high collisionality with a little to no-effect on plasma profiles [10]. In low collisionality and q_{95} discharges in AUG and KSTAR, however, a strong impact on kinetic profiles is observed, i.e. density pump-out and plasma braking. Although both cases (low/high densities) show a significant effect of the MPs on fast-ion losses, in low q_{95} and density / collisionality plasmas, MPs have a dramatic effect on fast-ion dynamics. We will report here on the effect of MPs on kinetic profiles including fast-ion dynamics in AUG. Dedicated experiments will be conducted in KSTAR in the following weeks, though preliminary results are in agreement with AUG observations.

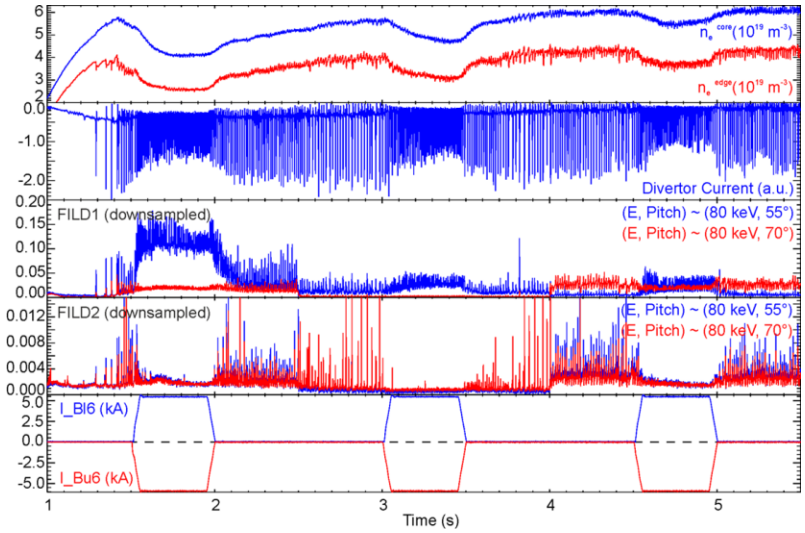

Fig.4. AUG discharge #28061. Overview of discharge with line integrated core and edge electron density, divertor current at outer target, fast-ion losses measured with FILD1 and FILD2 and timing of MP coil currents.

3.1. Plasma response to applied MPs

A series of plasma discharges with B_t = -2.5 T – -1.8 T, I_p= 0.8 MA, n_e ~ 5-6·10^{19}(m^{-3}) and a wide set of configurations of the external coils responsible for the MPs have been carried out in the AUG tokamak. Resonant and non(off)-resonant n=2 and n=3 coil configurations have been used to study the plasma response in low collisionality discharges. In plasmas with B_t = -2.5 T, the current of the coils was set at I_{coil} ~ 5.0 kA while for the discharges with B_t = -1.8 T, I_{coil} ~ 5.9 kA due to the weaker forces created in the coils with a lower B_t. The 3D dynamics of the plasma response to the applied MPs have been studied using the AUG comprehensive suite of plasma diagnostics (located at different positions) including Thomson Scattering (TS), Lithium beam, ECE, DCN, CXRS, 2D plasma imaging at different wave-lengths and MHD spectroscopy. In all discharges a significant density pump-out of up to 30 % is clearly observed and is typically accompanied by a marginal ELM mitigation. The electron and ion temperatures, T_e and T_i, are weakly affected and the strongest plasma braking is

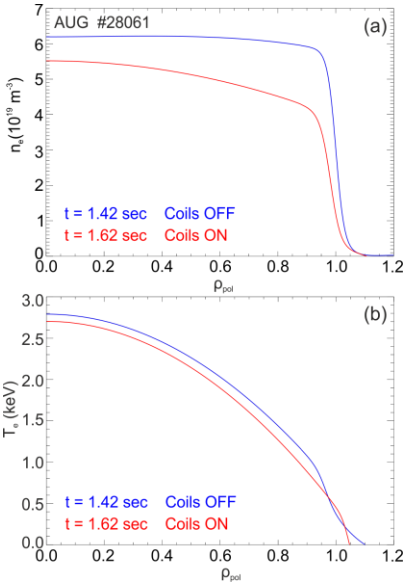

Fig.5. AUG discharge #28061. T_e and n_e profiles measured with and without MPs.

observed in the presence of a magnetic island with $n_{island}=n_{MP}$. Fig. 4 gives an overview of a typical discharge with a resonant n=2 MP configuration. T_e and n_e profiles measured with and without MPs are shown in Fig.5. As outlined in the previous, section a clear density pump-out is observed while T_e is not affected by the MPs. The effect of the density pump out is clearly visible in the beam emission too, see Fig. 6. The lower density during the MP phase leads to a deeper beam deposition and an apparent (large change in n_e but not in T_e) displacement of the separatrix of ~2-3 cm. MHD spectroscopy plays an important role when studying the plasma response to externally applied MPs and estimating the field penetration. In the present discharge a (3,2) NTM gets partially stabilized when applying the external MPs as it slows down in the background plasma. Fig. 7-(a) shows the spectrogram of a magnetic pick-up coil with the coils timing highlighted in white. A tangential beam (NBI#7), responsible for the higher nominal NTM frequency until t=4.0 sec, is replaced with a radial beam (NBI#5) with the corresponding drop in plasma rotation, visible in CXRS and the NTM frequency. The (3,2) NTM frequency drops up to ~30% when MP coils are switched on (with an apparent saturation frequency) achieving again rapidly its original nominal frequency when the MP coils are switched off. An estimation of the electromagnetic torque imposed by the coils' fields on the (3,2) magnetic island that seems to lead to this island braking will be the subject of a dedicated publication [24].

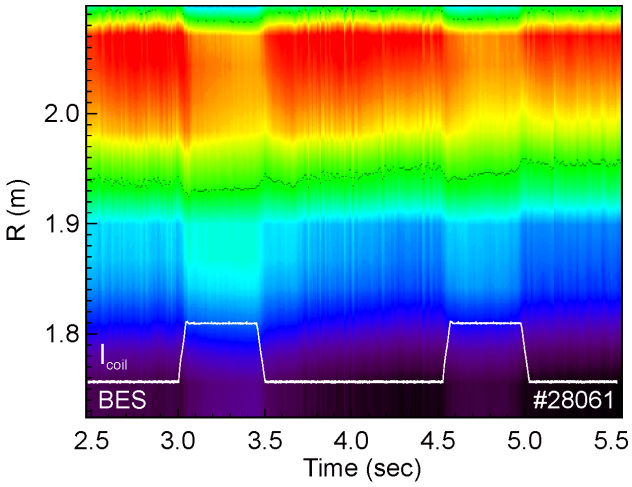

Fig.6. AUG discharge #28061. Beam emission measured with the AUG BES diagnostic.

3.2. Fast-ion dynamics in the presence of MPs

In AUG and KSTAR, the mitigation / suppression of type-I ELMs by externally applied MPs is often accompanied by a rather large loss of fast-ions with a broad-band frequency and amplitude correlated with the current of the MP coils. FILD measures at different locations an additional loss of fast-ions during the MP phase that can be up to an order of magnitude higher than the NBI prompt loss signal without MPs. The fast-ions response to MPs is, however, a complex 3D problem rather sensitive to the MP field penetration and overall plasma response. In the AUG discharge presented here, two FILD detectors were operating simultaneously with impressive differences in their signals. Fig. 4 shows the temporal evolution of the downsampled FILD1 and FILD2 signals. While FILD1 signals clearly rise when the coils are on, the FILD2 signals drop dramatically. The time traces of two

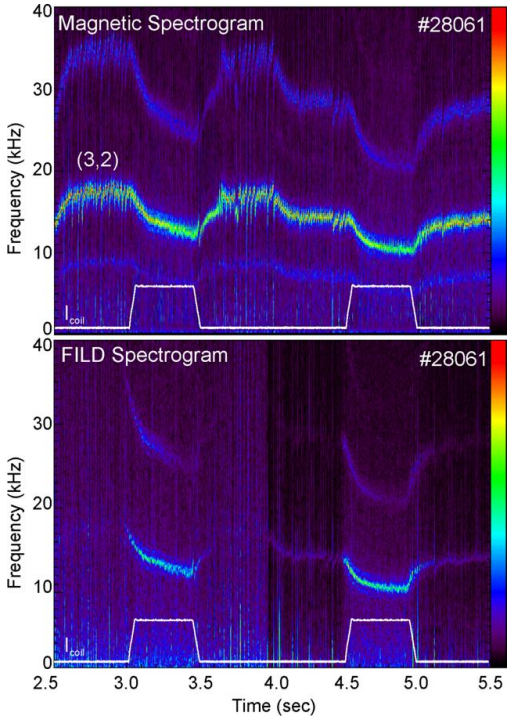

Fig.7. AUG discharge #28061. Spectrogram of (a) magnetic pick-up coil and (b) fast-ion losses measured by FILD1.

different pitch-angles and same energy (E ~ 80 keV) show some important differences in FILD1, with FILD2 signals having the same temporal evolution for both pitch-angles. A Fourier analysis of the fast-ion losses measured by FILD1 reveals that the (3,2) NTM is not causing any significant fast-ion loss without the MP coils though, during the MP phase, clear fast-ion losses correlated in frequency and phase with the internal (3,2) island are visible, see Fig.7-(b). The velocity-space of the escaping ions measured by FILD gives important information on the orbit topology of the ions that are most affected by the perturbation fields. In Fig. 8, the energy and pitch-angle of the escaping ions measured by FILD1 with and without the MP coils during the different NBI phases are shown. Fig.8-(a), coils OFF, and -(b), coils ON, correspond to the NBI#3+#8 phase. Fig.8-(c), coils OFF, and –(d), coils ON, correspond to the NBI#3+#7 phase and Fig.8-(e), coils OFF, and –(f), coils ON to the NBI#3+#5 phase. Fig.8-(a), -(c) and -(e) give an overview of the NBI prompt losses, with ~93 keV, measured by FILD1 while Fig.8-(b), -(d) and -(f) show the new velocity-space areas covered with fast-ion losses due to the MP coils. In all cases, fast-ion losses with gyroradii ~ 30-40 mm and pitch-angles ~ 60° appear only when the MP coils are ON. Fig.8-(b) and –(d) show, in addition, other energies and pitch-angles that without the MPs would be well confined. Most of the measured fast-ion losses are on banana orbits that explore the entire pedestal / SOL.

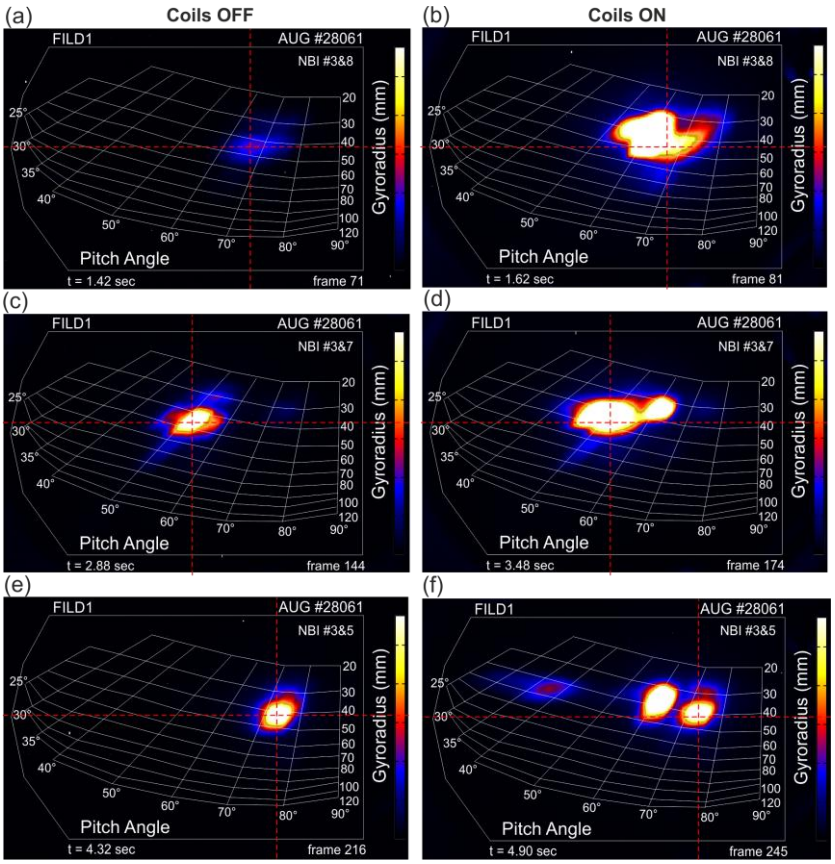

Fig.8. AUG discharge #28061. Velocity-space of escaping ions measured by FILD1 with MP coils OFF, (a), (c) and (e) and with MP coils ON, (b), (d) and (f).

The temporal evolution of the confined fast-ion profiles has been monitored with tangential and vertical active FIDA diagnostics. As the spectra covered by the tangential FIDA diagnostic includes the beam emission, one can infer a direct measure of the fast-ion content accounting for changes in beam deposition due to density pump out. Fig.9 shows the temporal evolution of the FIDA (a), beam emission (same as in Fig.6 but with less edge channels), (b), and fast-ion content, (c), profiles. A clear enhancement of the FIDA emission is visible when the MP coils are ON in both NBI phases. In fact, this enhancement of the FIDA emission is due to larger content of confined fast-ions during the MP phase and not only due to a deeper deposition of NBI neutrals as Fig.9-(c) shows with FIDA / BES. The lower collisionality due to density pump

out could account for the larger fast-ion content observed during the MP phases. If the MP fields are not efficiently screened by the plasma, the loss boundary may be moved inwards by the edge stochastic layer populating the loss cone with ions that would otherwise be well confined. Simulations of the experimental results presented here will be performed using MP fields calculated in vacuum as well as with different approaches for plasma shielding. In view of ITER, the detailed fast-ion measurements presented here will contribute to a better understanding of the interaction between fast-ions and MP fields and will likely constitute an important step towards the validation of plasma response and fast-ion transport codes. Special care should be taken in the possible impact that the MP-modified fast-ion profiles, in particular off-axis NBI profiles, may have in ITER MHD stability (including Alfven Eigenmodes) and first-wall localized heat load.

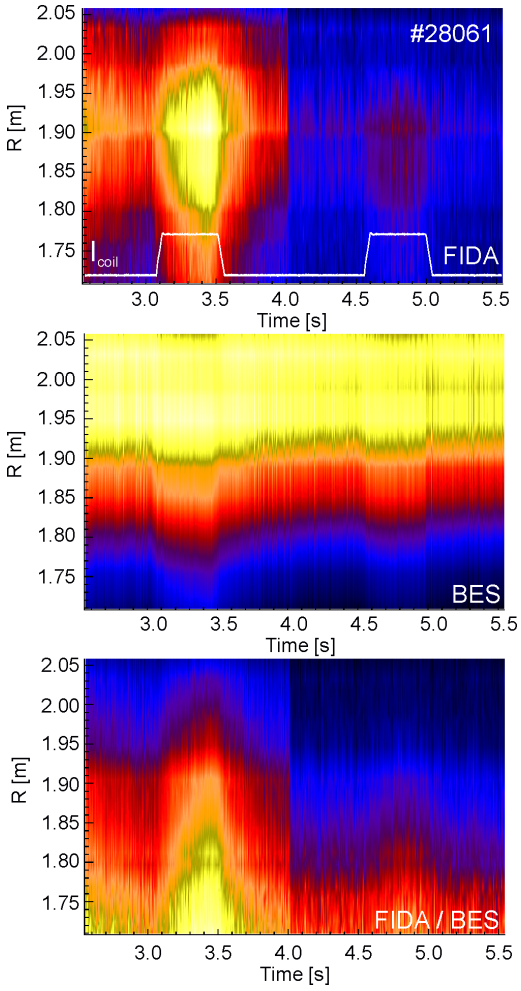

Fig.9. AUG discharge #28061. FIDA diagnostic. (a) FIDA emission, (b) Beam emission (BES), and (c) Fast-ion content (FIDA / BES).

References

[1] F. Wagner *et al.*, Phys. Rev. Lett. **49**, 1408 (1982)
[2] F. Wagner et al., Phys. Rev. Lett. 53, 1453 (1984)
[3] H. Zohm, Plasma Phys. Control. Fusion **38,** 105 (1996)
[4] G. Federici et al., Plasma Phys. Control. Fusion **45,** 1523 (2003)
[5] A. Loarte et al., Plasma Phys. Control. Fusion **45**, 1549 (2003)
[6] R. A. Pitts et al., J. Nucl. Mater. **363**, 1093 (2011)
[7] P. B. Snyder et al., Nucl. Fusion **44,** 320 (2004)
[8] T. C. Hender et al., Nucl. Fusion **32**, 2091 (1992)
[9] Y. Liang et al., Phys. Rev. Lett. **98**, 265004 (2007)
[10] T. E. Evans et al., Phys. Rev. Lett. **92**, 235003 (2004)
[11] W. Suttrop et al., Phys. Rev. Lett. **106**, 225004 (2011)
[12] M. Okabayasi et al., Nucl. Fusion **45**, 1715 (2005)
[13] Q. Hu et al., Nucl. Fusion **52,** 083011 (2012)
[14] R. J. La Haye et al., Phys. Plasmas **9**, 2051 (2002)
[15] A. B. Rechester and M. N. Rosenbluth, Phys. Rev. Lett. **40**, 38 (1978)
[16] J. A. Heikinnen and J. Lönnroth, Plasma Phys. Control. Fusion 49, B465-B477 (2007)
[17] A. D. Turnbull, Nucl. Fusion **52,** 054016 (2012)
[18] M. Kocan et al., this conference, EX / P7-23
[19] M. Garcia-Munoz et al., Rev. Sci. Instrum. **80**, 053503 (2009)
[20] R. K. Fisher *et al.*, Rev. Sci. Instrum. **81**, 10D307 (2010)
[21] J. Kim et al., Rev. Sci. Instrum. **83**, 10D305 (2012)
[22] W. W. Heidbrink et al., Plasma Phys. Contr. Fusion **46,** 1855 (2004)
[23] B. Geiger et al., Plasma Phys. Contr. Fusion **53,** 065010 (2011)
[24] S. Fietz et al., in prep.

Acknowledgement

This work was supported in part by the US Department of Energy under SC-G903402, DE-FC02-04ER54698, DE-FG02-99ER54531, and DE-FG02-08ER54984.